Volume 50(11): 1525–1536, 2002
The Journal of Histochemistry & Cytochemistry
http://www.jhc.org

ARTICLE

Specific Responses in Rat Small Intestinal Epithelial mRNA Expression and Protein Levels During Chemotherapeutic Damage and Regeneration

Melissa Verburg, Ingrid B. Renes, Danielle J.P.M. Van Nispen, Sacha Ferdinandusse, Marieke Jorritsma, Hans A. Büller, Alexandra W.C. Einerhand, and Jan Dekker

Pediatric Gastroenterology and Nutrition, Department of Pediatrics, Erasmus University (MV,IBR,DJPMVN,SF,MJ,AWCE,JD) and Sophia Children's Hospital (HAB), Rotterdam, The Netherlands

SUMMARY The rapidly dividing small intestinal epithelium is very sensitive to the cytostatic drug methotrexate. We investigated the regulation of epithelial gene expression in rat jejunum during methotrexate-induced damage and regeneration. Ten differentiation markers were localized on tissue sections and quantified at mRNA and protein levels relative to control levels. We analyzed correlations in temporal expression patterns between markers. mRNA expression of enterocyte and goblet cell markers decreased significantly during damage for a specific period. Of these, sucrase-isomaltase (−62%) and CPS (−82%) were correlated. Correlations were also found between lactase (−76%) and SGLT1 (−77%) and between I-FABP (−52%) and L-FABP (−45%). Decreases in GLUT5 (−53%), MUC2 (−43%), and TFF3 (−54%) mRNAs occurred independently of any of the other markers. In contrast, lysozyme mRNA present in Paneth cells increased (+76%). At the protein level, qualitative and quantitative changes were in agreement with mRNA expression, except for Muc2 (+115%) and TFF3 (+81%), which increased significantly during damage, following independent patterns. During regeneration, expression of each marker returned to control levels. The enhanced expression of cytoprotective molecules (Muc2, TFF3, lysozyme) during damage represents maintenance of goblet cell and Paneth cell functions, most likely to protect the epithelium. Decreased expression of enterocyte-specific markers represents decreased enterocyte function, of which fatty acid transporters were least affected.
(J Histochem Cytochem 50:1525–1536, 2002)

KEY WORDS
methotrexate
intestinal function
malabsorption
diarrhea

The use of the cytostatic drug methotrexate (MTX) in anti-cancer treatments severely impairs intestinal epithelial function, which constitutes a major dose-limiting factor in treatment schedules (Fata et al. 1999; Kohout et al. 1999). Like γ-irradiation, this drug induces diarrhea and anorexia, which is associated with malabsorption, malnutrition, and dehydration (Pinkerton et al. 1982). It is of great importance to unravel the response of the small intestinal epithelium to cytostatic agents at the biochemical level so as to gain insight in the functional properties of the epithelial cells during damage and subsequent regeneration.

As a folic acid analogue, the action of MTX primarily inhibits DNA synthesis by binding to the enzyme dihydrofolate reductase (Werkheiser 1961). This leads to an inhibition of proliferation in the crypts of the small intestine (Goldman and Matherly 1985). It has been demonstrated in biopsy specimens from human cancer patients that epithelial damage in the small intestine caused by chemotherapy can be identified via increases in apoptosis in the crypts, epithelial changes in cell height and crypt height, and the manifestation of villous atrophy (Keefe et al. 2000).

In our rat model of chemotherapeutic damage and

Correspondence to: Dr. Jan Dekker, Laboratory of Pediatrics, Room Ee1571A, Erasmus University, Dr Molewaterplein 50, 3015GE Rotterdam, The Netherlands. E-mail: dekker@kgk.fgg.eur.nl

Received for publication November 21, 2001; accepted June 5, 2002 (1A5686).

0022-1554/02/$3.30

regeneration in the small intestinal epithelium, four phases could be discriminated after the two-dose administration (IV) of 20 mg/kg plus 10 mg/kg body weight MTX (Verburg et al. 2000). In this model, days 1 and 2 represented damage in the crypt epithelium, which was characterized by increased apoptosis as well as decreased crypt depth and cell height. Days 3 and 4 represented a phase of prominent damage to the villous epithelium, marked by reduced cell and villous heights as well as accumulating goblet cells at the tips of the small intestinal villi. Days 5 and 6 represented a phase of regeneration via increased proliferation during which the morphological appearance of the epithelial cells returned to normal. Days 8 and 10 represented a phase of regenerated small intestinal epithelium, which was indistinguisable from that of untreated rats (Verburg et al. 2000).

Studies have been performed with the use of particular growth factors, such as TGF (Booth et al. 2000), KGF (Booth and Potten 2001), EGF (Petschow et al. 1993; Hirano et al. 1995) and IGF (Howarth et al. 1998), that aimed to protect the small intestinal epithelium against radiation injury or damage by cytostatic drugs. For example, the prophylactic administration of transforming growth factor β (TGFβ) was able to decrease proliferation in the stem cell region before radiation injury, which resulted in enhanced crypt survival and enhanced recovery in mice (Booth et al. 2000). In addition, therapeutic administration, but not prophylactic administration, of epidermal growth factor (EGF), insulin-like growth factor (IGF-I), and TGFβ has been shown to stimulate epithelial proliferation in the regeneration phase after radiation- or MTX-induced injury in mice (Petschow et al. 1993; Hirano et al. 1995; Potten et al. 1995; Howarth et al. 1998). Therefore, although these growth factors are important for enhanced recovery of the small intestinal epithelium, they fail to prevent or reduce the development of the initial damage.

The functions of intestinal epithelial cells are reflected by the expression of cell type-specific genes. Very little is known about the absorptive and protective functions of epithelial cells during damage and regeneration induced by chemotherapy. Sucrase–isomaltase and lactase, responsible for intestinal disaccharidase activities, were decreased during MTX-induced damage in rat small intestine (Taminiau et al. 1980; Kralovanszky and Prajda 1985). In contrast, the amino acid transporter Pept1 appeared resistant to damage in the ileum of 5′-fluorouracil (5-FU)-treated rats (Tanaka et al. 1998). Furthermore, MTX-treatment appeared to affect the various populations of epithelial cell types differently. Relative to enterocytes, epithelial goblet and Paneth cells were spared from cell death in rat small intestine after MTX treatment (Verburg et al. 2000). Very little is known about the contribution of these specialized cell types to epithelial protection during such a response.

In the present study, the functional capacities of the epithelial cells were investigated during MTX-induced damage and repair, through analysis of the expression of a range of differentiation markers. The following markers were used for enterocytes: carbamoylphosphate synthase (CPS), sucrase–isomaltase (SI), lactase, glucose transporter-5 (GLUT5), sodium glucose co-transporter 1 (SGLT1), intestinal- and liver fatty acid-binding protein (I-FABP and L-FABP, respectively). For goblet cells the markers mucin (MUC2) and trefoil factor 3 (TFF3) were investigated and lysozyme was used to study Paneth cell function. The jejunum was chosen as a representative for the small intestine, because morphology and proliferation were similarly affected along the small intestinal axis in this model (Verburg et al. 2000). Epithelial gene expression was quantified at the mRNA and protein levels and compared with the immunohistochemical localization of the protein at sequential days after MTX treatment.

Materials and Methods

Animals

Six-week-old male Wag/Rij rats (Broekman; Utrecht, The Netherlands) were kept under specific pathogen-free conditions with free access to water and defined semi-synthetic chow (Hope Farms; Woerden, The Netherlands). Glucose, starch, and cellulose constitute the carbohydrates in the food: 424 g/kg, 140 g/kg, and 45 g/kg, respectively. On analysis, no other carbohydrates were found. The folic acid content was 0.98 mg/kg. The dosage schedule of MTX treatment was defined during pilot studies. At day −1, 20 mg/kg body weight methotrexate (MTX, Ledertrexate SP forte; Cyanamid Benelux, Etten-Leur, The Netherlands) was injected IV under light anesthesia. At 24 hr later (day 0), a second injection of 10 mg/kg body weight MTX was given. Control animals received equivalent volumes of 0.9% (w/v) sodium chloride solution both times. At days 1, 2, 3, 4, 5, 6, 8, and 10 after the second dose of MTX, three rats were sacrificed by decapitation after anesthesia. Three control animals were sacrificed at day 8. The experiments were performed with permission of the Animal Ethics Committee of our institution. Jejunal segments (anatomic middle of the small intestine) were rinsed in PBS, fixed in 4% (w/v) paraformaldehyde (Merck; Darmstadt, Germany) in PBS, and processed for immunohistochemistry according to standard procedures (Verburg et al. 2000). In addition, adjacent intestinal segments (0.5 cm long) were frozen in liquid nitrogen and stored at −80C for quantitative mRNA and protein analysis.

Immunohistochemistry

Expression and localization of protein were detected using immunohistochemistry according to standard procedures (Verburg et al. 2000). Antigen unmasking was carried out by heating the sections for 10 min in 0.01 M sodium citrate

(pH 6.0) at 100C. Endogenous peroxidase activity was blocked by treatment with 1.5% H_2O_2 in PBS for 30 min. Nonspecific protein binding was blocked using a buffer containing 10 mM Tris (pH 8.0), 5 mM ethylenediamine tetraacetic acid (Merck), 0.15 M NaCl (Fluka Chemie; Zwijndrecht, The Netherlands), 0.25% (w/v) gelatin (Merck), and 0.05% (w/v) Tween-20 (Merck). All sections were incubated overnight at 4C using one of the primary antibodies diluted in PBS (Table 1). The antibodies raised against human SGLT1 (Yoshida et al. 1995), human MUC2 (Tytgat et al. 1995a,b), and human lysozyme (Dako; Glostrup, Denmark) were shown to be specific in rat. Antibody binding was visualized using biotin-labeled secondary antibodies and Vectastain, an avidin–biotin–peroxidase complex detection kit, according to the manufacturer's instructions (Vector Laboratories; Burlingame, CA). All sections were recorded and analyzed using a CCD camera (Sony) and an Eclipse E800 Microscope (Nikon; Tokyo, Japan). Appropriate control staining was performed, leaving out each of the primary antibodies, which resulted in complete absence of staining for each separate antibody at the dilutions used in our experiments (Table 1).

mRNA Quantitation

Total RNA was isolated from frozen tissue using Trizol reagent (Gibco-BRL; Gaithersburg, MD). Ten μg of total RNA was run on 1% or 1.2% (w/v) agarose gels containing 0.5 M glyoxal (Boehringer Mannheim; Mannheim, Germany) and blotted overnight onto Hybond-N+ membranes (Amersham; Poole, UK). Serial dilutions of each RNA sample were analyzed to ensure that the mRNA quantification, of each marker mRNA, using its cognate cDNA probe, was performed within the linear range of this technique. All blots were baked for 2 hr at 80C and hybridized using rat-specific, $\alpha[^{32}P]$-dATP-labeled cDNA probes. The following rat-specific cDNA probes were used: CPS (Nyunoya et al. 1985), SI (Krasinski et al. 1994), lactase (Büller et al. 1990), SGLT1 (Burant et al. 1994), GLUT5 (Rand et al. 1993), I-FABP (Alpers et al. 1984), L-FABP (Gordon et al. 1983), MUC2 (Verburg et al. 2000), TFF3 (Suemori et al. 1991), and lysozyme (Yogalingam et al. 1996). Each probe hybridized to an mRNA band of the appropriate molecular weight as originally described for the respective probes. Moreover, all bands were clear and discrete, and no signs of RNA degradation were observed. After exposure for 1 or 2 days to PhosphorImager plates, the hybridization signals were quantified using a PhosphorImager and ImageQuant software (Molecular Dynamics/Amersham; Roosendaal, The Netherlands). Expression was corrected for the amount of glyceraldehyde-3-phosphate dehydrogenase (GAPDH) mRNA, which served as internal standard.

Protein Quantitation

Changes in epithelial protein expression were determined in tissue homogenates using quantitative Western blotting. Tissue was homogenized in HEPES buffer [20 mM HEPES (Merck), pH 7.5, 20 mM NaCl (Boehringer), 0.5% (w/v) Triton X-100 (BDH; Poole, UK)] containing 10 μg/ml pepstatin A (Sigma; St Louis, MO), 10 μg/ml leupeptin (Sigma), 1 mM phenylmethylsulfonyl fluoride (Sigma), and 0.38 U/ml aprotinin (Sigma) as protease inhibitors, using a Polytron (Kinematica AG; Basel, Switzerland). Ten μg of total protein was separated on 7% or 15% (w/v) SDS-PAGE and blotted for 1 hr onto Hybond+ membranes. Serial dilution series of the protein samples were analyzed to ensure that the quantification of each protein by its cognate antibody was performed in the linear range of this technique. Routine staining of the SDS-PAGE gels for protein after blotting showed complete transfer of the proteins to the membrane. After incubation for 1 hr in blocking buffer [Tris pH 7.8 (Merck), 2 mM $CaCl_2$ (Merck), 5% (w/v) low-fat milk powder (Nutricia; Wageningen, The Netherlands), 0.05% (w/v) Triton X-100 (BDH), and 0.05% (v/v) Antifoam (Sigma)], the blots were incubated overnight at 4C with one of the primary antibodies (Table 1). After rinsing in blocking buffer, the blots were incubated for 2 hr in blocking buffer, containing 0.1 μCi/ml ^{125}I-labeled protein A (Amersham). After rinsing three times in Tris buffer (pH 7.8), the blots were dried and exposed to PhosphorImager plates for 3 days. Each individual protein marker yielded clear and reproducible protein bands at the expected molecular weight as described in the original publications (Table 1). Signals were quantified as described above.

Table 1 Antibodies to detect intestinal epithelial proteins[a]

Antigen	Dilution		Type
	Western Blotting	IHC	
Rat CPS	1:1000	1:5000	r-polyclonal (Gaasbeek Janzen et al. 1984)
Rat SI[b]	—	1:6000	r-polyclonal (Yeh et al. 1991)
Rat SI[b]	1:100	—	m-monoclonal (Quaroni and Isselbacher 1985)
Rat GLUT5	1:500	1:1000	r-polyclonal (Rand et al. 1993)
Rat I-FABP	1:1000	1:4000	r-polyclonal (Rubin et al. 1989)
Rat L-FABP	1:1000	1:4000	r-polyclonal (Rubin et al. 1989)
Rabbit SGLT1	—	1:1000	m-monoclonal (Hwang et al. 1991)
Rat MUC2[b]	1:1000	—	r-polyclonal (Tytgat et al. 1995b)
Human MUC2[b]	—	1:100	m-monoclonal (Podolsky et al. 1986)
Rat TFF3	1:200	1:6000	r-polyclonal (Suemori et al. 1991)
Human lysozyme	—	1:50	r-polyclonal (this study)

[a]Each antibody was shown to be specific in rat (see Materials and Methods for additional references).
[b]Except for SI and MUC2, the same antibodies were used for both Western blotting and immunohistochemistry. r, rabbit; m, mouse.

Statistical Analysis

Changes in mRNA and protein expression levels during damage and regeneration were statistically analyzed using the Mann–Whitney *U*-test. The statistical correlation coefficient (rho) between mRNA and protein expression and between morphological parameters and mRNA/protein expression was analyzed using Spearman's test, based on data from the individual rats. Similarly, correlation coefficients between the various mRNAs/proteins were used to study coordinate gene expression. In all tests, $p<0.05$ was considered statistically significant.

Results

The Model

Using this animal model, we have shown previously that we could induce characteristic cytotoxic damage to the intestinal epithelium of rats by a 2-day treatment with MTX (Verburg et al. 2000). As noted in this previous study, the pattern of damage and regeneration varied slightly among individual animals. As it appeared, data were most clearly presented by pooling the data obtained from animals of two consecutive time points to correct for the observed temporal variations. Data are presented from four characteristic windows in the course of damage and regeneration, as described earlier (Verburg et al. 2000). Days 1–2 after the last MTX injection were characterized as a period of inhibited proliferation, severe cell damage in the small intestinal crypt epithelium, and decreased crypt depth. Villous height was slightly decreased, but the villous epithelial cells appeared normal. Days 3–4 were characterized by hyperproliferation, crypt regeneration, and villous atrophy. The villous epithelial cells were depleted and appeared flattened. During days 5–6, villous regeneration occurred, whereas proliferation gradually returned to normal. Regeneration was complete on days 8–10.

Basically, the response to MTX was similar in each region of the small intestine (Verburg et al. 2000, and results not shown). Therefore, only representative data of the jejunum are shown here. There were no macroscopic or microscopic lesions in the epithelium at any time during the course of damage and regeneration (not shown). It should therefore be noted that the epithelial barrier was not breached and there was no apparent denuding of the mucosa during the experiment. This was particularly relevant for the changes in the expression patterns of the enterocyte markers, which were basically expressed within the same villous epithelial cells. Therefore, the relative changes in quantitative gene expression patterns of the individual markers were measures of specific gene regulation under these circumstances. In addition, it is noteworthy that the correlation analyses between quantitative data regarding gene expression were calculated using the data for each marker of the individual animals.

Enterocytes

Immunohistochemistry was performed to study the fate of enterocytes during the experiment and to localize enterocyte-specific protein expression. Because a very sensitive but non-linear detection method was used to visualize binding of antibodies, staining intensities were not quantitatively interpreted throughout the study. In control rats, CPS protein was expressed in a mosaic pattern and was localized in series of adjacent enterocytes both in crypt and in the villous epithelium (Figure 1A). On days 1–2 most of the crypts were not stained for CPS, but the protein was still present in the villous region (Figure 1B). On days 3–4, CPS protein expression was less abundant on the villi compared to controls and rats of days 1–2. Part of the enterocytes on the villous tips showed CPS immunoreactivity during this period of severe villous damage, but the crypt and villous enterocytes were mostly CPS-negative (Figure 1C). On days 5–6, the mosaic pattern of CPS had returned on part of the villi, and the expression pattern was fully restored on days 8–10 (Figure 1D).

SI was found in the brush border and in the Golgi region of villous enterocytes in control rats (Figure 1E). The estimated number of SI-positive villous cells decreased according to the length of the villi, and during the phase of damage on days 1-4 the intracellular Golgi staining was absent (Figures 1F and 1G). Very few SI-positive cells were seen on days 3–4, during maximal villous damage on the tips of the rudimentary villi (Figure 1G). As the villi increased in length during regeneration, the localization of SI-positive cells returned to normal (Figure 1H).

Like SI, GLUT5 and SGLT1 proteins were localized in the brush border of villous enterocytes in control tissue (Figures 1I and 1M). The estimated numbers of GLUT5- and SGLT1-positive villous enterocytes decreased gradually towards the tips of the shortening villi during days 1–4 until both markers were unde-

Figure 1 Immunohistochemical detection of proteins expressed in jejunum enterocytes during different phases of MTX-induced damage and regeneration. The following enterocyte-specific proteins were detected; CPS (**A–D**), SI (**E–H**), GLUT5 (**I–L**), SGLT1 (**M–P**), I-FABP (**Q–T**), and L-FABP (**U–X**). (**A,E,I,M,Q,U**) Control sections. (**B,F,J,N,R,V**) Sections at 2 days after MTX treatment. (**C,G,K,O,S,W**) Sections at 4 days after MTX treatment. (**D,H,L,P,T,X**) Tissue 8 days after MTX treatment. Arrows in **E** and **H** indicate staining of the Golgi complex by the anti-SI antibodies. Bar = 200 μm.

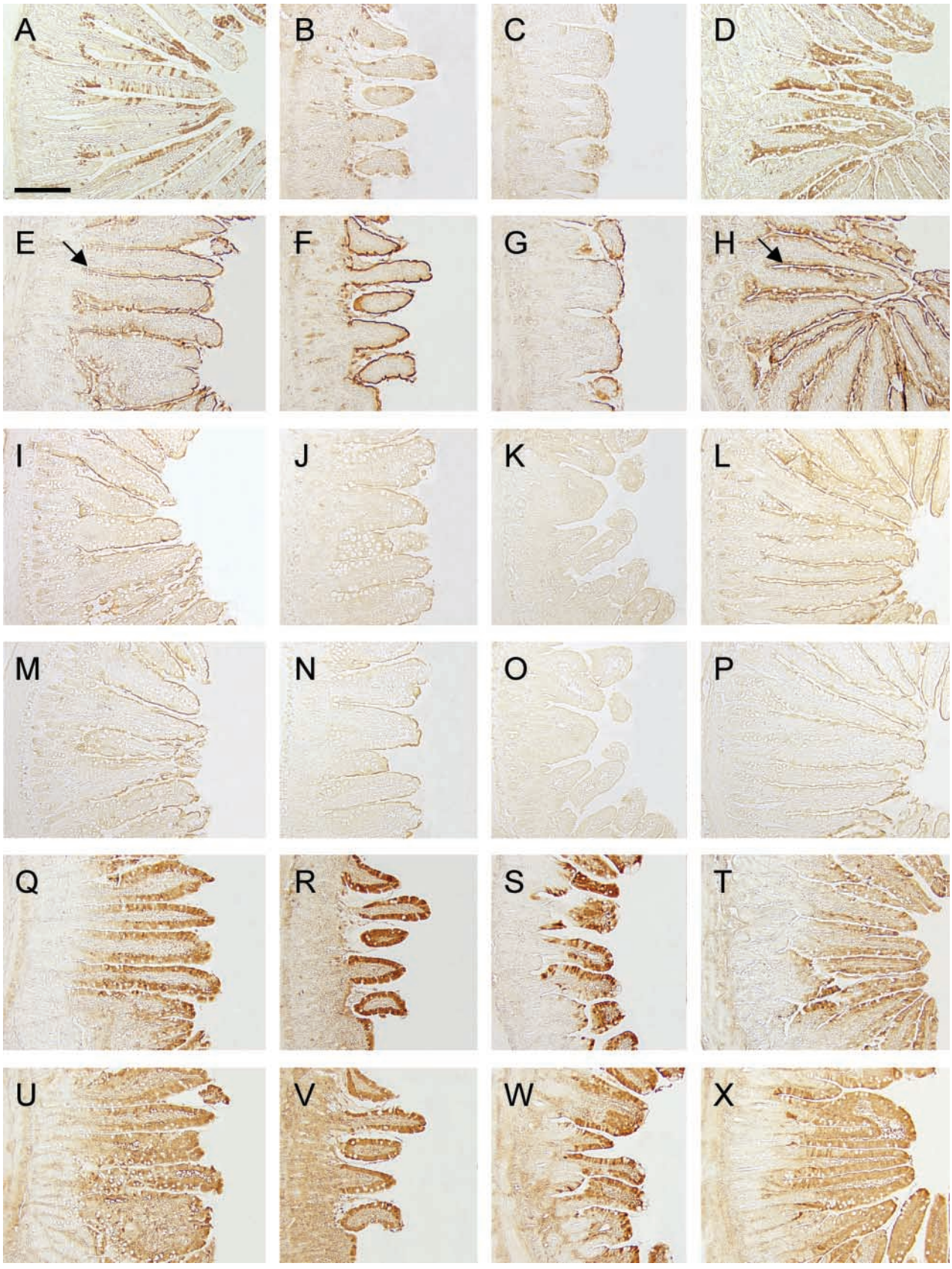
A
B
C
D
E
F
G
H
I
J
K
L
M
N
O
P
Q
R
S
T
U
V
W
X

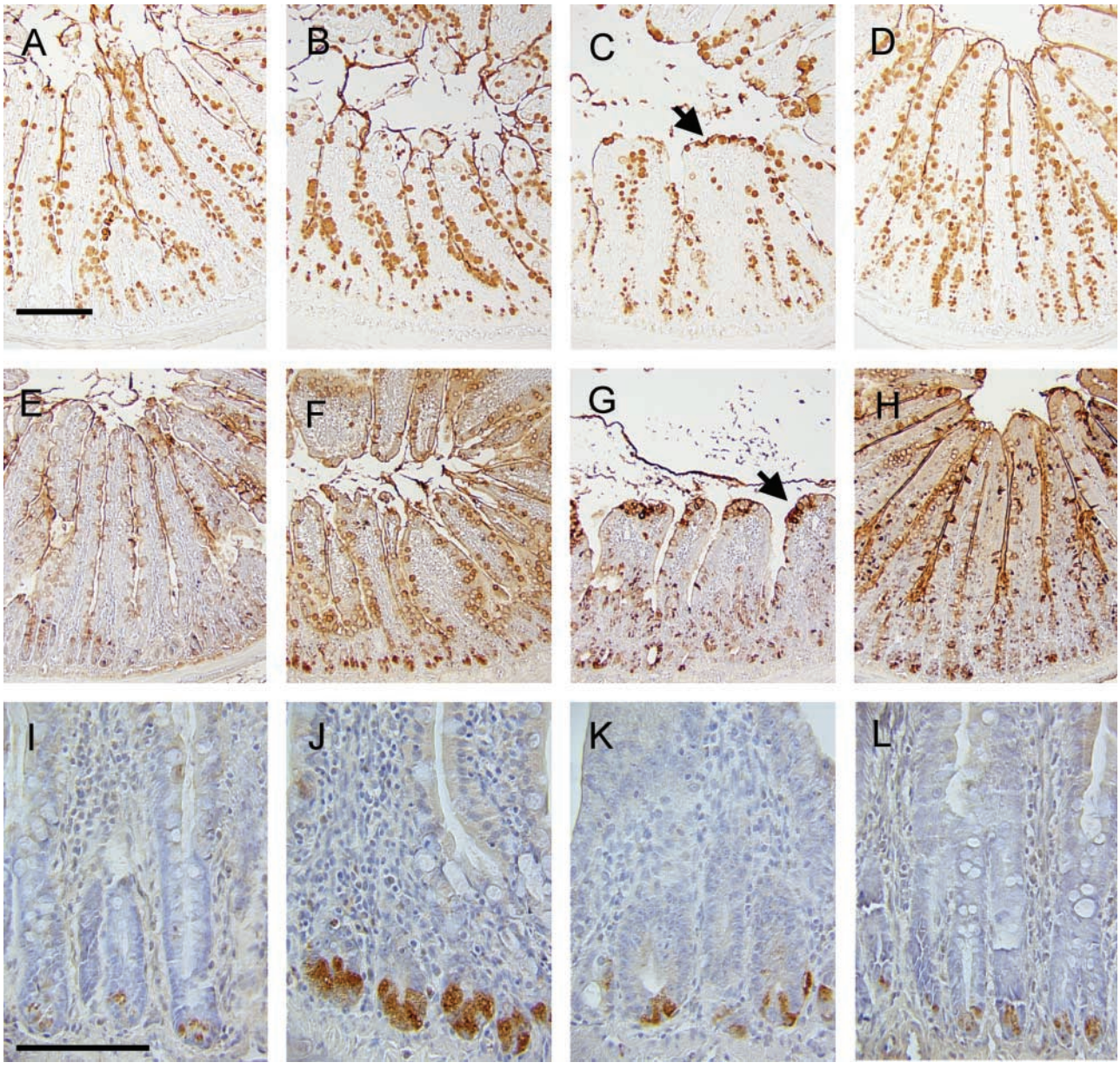

Figure 2 Immunohistochemical detection of proteins expressed in jejunum goblet or Paneth cells during different phases of MTX-induced damage and regeneration. MUC2 (**A–D**) and TFF3 (**E–H**) were detected in goblet cells, whereas lysozyme (**I–L**) was detected in Paneth cells. (**A,E,I**) Control sections. (**B,F,J**) Sections at 2 days after MTX treatment. (**C,G,K**) Sections at 4 days after MTX treatment. (**D,H,L**) Tissue 8 days after MTX treatment. Arrows in **C** and **G** indicate goblet cells accumulated at the tips of the rudimentary villi 4 days after MTX treatment. Sections in **E–L** were briefly stained with hematoxylin. Bars: **A** = 200 μm; **I** = 100 μm.

tectable on day 4 (Figures 1K and 1O). From day 6 onwards, expression patterns of SGLT1 and GLUT5 were similar to those found in controls (Figures 1L and 1P).

I-FABP and L-FABP expression was localized in the cytoplasm of all villous enterocytes in controls (Figures 1Q and 1U). MTX-induced changes in expression were similar for both FABP proteins. These changes were much less pronounced than for the brush border markers SI, GLUT5, and SGLT1. Despite the increasing villous cell damage up to 4 days after MTX treatment, I-FABP and L-FABP immunostaining remained present in enterocytes of the remaining villous enterocytes (Figures 1R, 1S, 1V, and 1W). As in controls, I-FABP and L-FABP were expressed in all villous enterocytes on days 5–10 (Figures 1T and 1X).

Lactase mRNA levels could be detected as an enterocyte marker, but lactase protein could not be lo-

calized using the available antibodies because of its very low expression levels in these adult rats (Rings et al. 1994, and data not shown).

Goblet and Paneth Cells

The fate of goblet and Paneth cells was studied by immunohistochemistry for secretory products produced specifically by these cells. In contrast to the enterocyte markers, the markers for these cell types appeared to largely persist throughout the course of damage and regeneration. MUC2 was stained in the goblet cells at all time points during the experiment, and MUC2-positive goblet cells were also expressing TFF3 (Figure 2). The estimated number of MUC2- and TFF3-positive cells was decreased compared with controls during days 1–2 along the crypt–villous axis during the increasing villous atrophy (Figures 2B and 2F). This was followed around day 4 by a depletion of MUC2- and TFF3-positive cells in the lower villous region and an accumulation of MUC2- and TFF3-positive cells in the villous tip region (Figures 2C and 2G). During regeneration, MUC2 and TFF3 expression became comparable with controls (Figures 2D and 2H).

Paneth cells in the crypts were lysozyme-positive at all days analyzed. A transient induction of lysozyme immunostaining was seen during crypt damage on days 1–2 (Figures 2I and 2J), which gradually returned to normal staining patterns on days 3–4 and beyond (Figures 2K and 2L).

Expression of Enterocyte-specific mRNAs

The expression of cell type-specific mRNA was quantified by Northern blotting for each individual rat, as shown in Figure 3A. Pooling of quantitative data from two consecutive time points was performed to minimize intra-animal variations and to accentuate the differences between markers during the course of damage and regeneration (Figure 4).

The changes in mRNA expression of each enterocyte marker had a characteristic pattern in time (Figure 4A). However, the level of each enterocyte mRNA returned to levels that were not significantly different from control levels at days 8–10 after MTX treatment. We performed correlation analysis on changes in the mRNA levels of these markers on the data from each individual animal. Four types of patterns could be distinguished, based on temporal differences in sensitivity to MTX treatment. Within each type, the expression patterns of the markers were highly correlated, whereas there were no statistically significant correlations with the expression patterns of the markers from any other type. We could distinguish type 1, CPS and SI; type 2, SGLT1 and lactase; type 3, I-FABP and L-FABP; and type 4, GLUT5 (Figure 4). Of these, CPS and SI mRNAs were most affected at an early stage. During minimal crypt depth on days 1–2, levels of CPS and SI mRNA

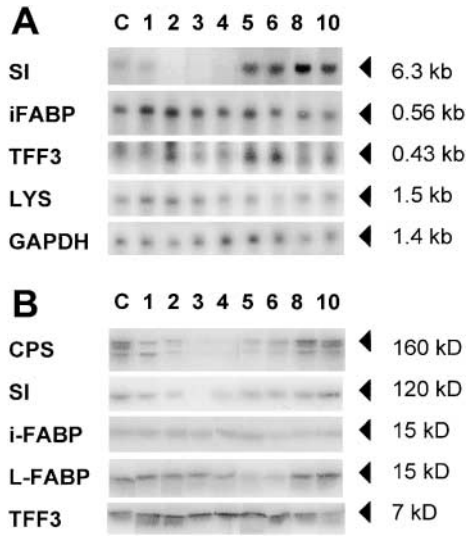

Figure 3 Representative Northern blots (**A**) and Western blots (**B**) demonstrating the expression of selected small intestinal markers. Days after MTX treatment are indicated above the graphs. C, control. All results are shown for one rat at each time point. At right are the sizes of the mRNA (in kilobases, **A**) and the proteins (in kilodaltons, **B**).

expression were 82% and 62% decreased, respectively, compared with controls (Figure 4A). During maximal villous damage on days 3–4, CPS and SI were still significantly decreased, but the levels recovered relatively rapidly compared to the other markers.

SGLT1 and lactase mRNA levels were the most affected at a later stage, at maximal villous damage on days 3–4 and recovered more slowly compared to CPS and SI (Figure 4A). The expression of SGLT1 and lactase mRNA was already significantly decreased on days 1–2 compared with control (−50%). This decrease progressed to days 3–4, when SGLT1 and lactase mRNAs were hardly detectable (−77% and −76%, respectively). In contrast to CPS and SI mRNAs, SGLT1 and lactase mRNAs were still significantly decreased on days 5–6.

I-FABP and L-FABP mRNA levels were markedly less affected than the previous four markers and were first significantly affected at maximal villous damage, whereas the mRNA levels recovered relatively late and more slowly compared to CPS, SI, SGLT1, and lactase (Figure 4A). Expression levels of I-FABP and L-FABP mRNAs decreased significantly on days 3–4 at 52% and 45%, respectively (Figure 4A). As for SGLT1 and lactase, regeneration within the tissue was not immediately associated with a normalization of I-FABP and L-FABP mRNA expression, because both markers were still significantly decreased on days 5-6.

In contrast to all other enterocyte markers, the mRNA levels of GLUT5 were only affected significantly

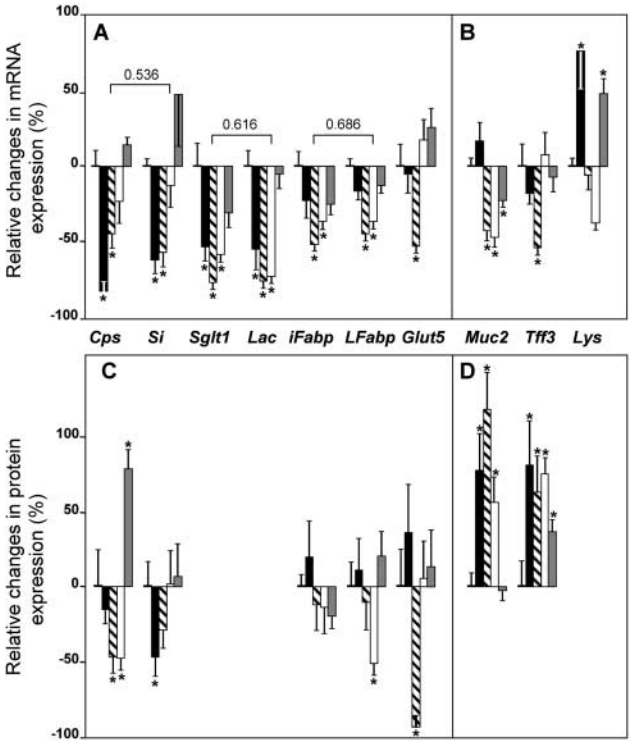

Figure 4 Relative changes in epithelial mRNA and protein expression in the jejunum after MTX treatment. Panels indicate the mRNA levels of enterocyte (**A**) and of goblet and Paneth cell markers (**B**) as detected by Northern blotting, and of the protein levels of enterocyte (**C**) and of goblet and Paneth cell markers (**D**) as detected through Western blotting. Control levels, defined as 100%, were set at 0 on the horizontal axis. The relative in-/decrease, expressed as percentage of control levels, was analyzed on days 1–2 (black bars), days 3–4 (crosshatched bars), days 5–6 (open bars), and days 8–10 (gray bars). Closely correlated expression patterns could be distinguished in enterocyte-specific mRNAs as indicated by brackets (indicated is the correlation coefficient rho, according to Spearman's test): between CPS and SI (rho=0.536; p=0.008), between SGLT1 and lactase (rho=0.616; p=0.001), and between I-FABP and L-FABP (rho=0.686; p<0.0005). LAC, lactase, LYS, lysozyme. Error bars indicate SEM. Asterisks indicate statistically significant differences relative to control levels at p<0.05.

during one specific phase of disease, i.e., at maximal villous damage (days 3–4, −53%), and recovered rapidly during regeneration (Figure 4A).

We analyzed the relations between the level of expression of each marker and the crypt depth and villous atrophy, measured as described previously (Verburg et al. 2000). CPS and SI mRNA expression levels were correlated to changes in crypt depth (rho=0.399 and rho=0.432, respectively; p<0.05) as well as villous height (rho=0.377 and rho=0.483, respectively; p<0.05). The temporal patterns of expression levels of lactase, GLUT5, SGLT1, I-FABP, and L-FABP mRNA did not correlate with the variations in crypt depth or villous height.

Expression of Goblet and Paneth Cell-specific mRNAs

The response of each of the markers for the goblet and Paneth cells was very specific and was different from any of the changes seen for the enterocyte markers (Figures 3A and 4A). MUC2 mRNA expression was significantly but inversely correlated to crypt depth (rho=−0.610; p=0.001). During early damage on days 1–2, MUC2 mRNA levels remained stable. Thereafter, MUC2 mRNA levels were significantly decreased and remained below control levels up to days 8–10 (Figure 4B). MUC2 and TFF3 protein co-localized to the same cells (Figure 2). Interestingly, though, TFF3 mRNA levels were not significantly correlated to MUC2 mRNA levels. TFF3 mRNA levels were decreased only on days 3–4 relative to controls (Figure 4B).

Lysozyme mRNA levels were significantly increased (+76%) at early stages of damage on days 1–2 (Figure 4B), in agreement with the immunohistochemical localization of the protein (Figure 2J), and were rapidly normalized on days 3–6. There was no significant correlation with any of the morphological parameters. Surprisingly, a second induction of lysozyme mRNA levels occurred on days 8–10 (Figure 4B) despite the seemingly normal lysozyme protein expression at the immunohistological level (Figure 2L).

Expression Levels of Epithelial Proteins

Temporal expression patterns of epithelial proteins were quantified on Western blots, as illustrated in Figure 3B, and compared with expression patterns of the encoding mRNAs. Despite our efforts we were not able to quantify the protein levels of all markers. Therefore, we were not able to quantify SGLT1, lactase, and lysozyme protein due to lack of antibodies that were able to reproducibly detect these antigens on Western blotting.

The protein expression level of each enterocyte marker showed a specific pattern in time. Correlation analysis, determined from the data of the individual rats, revealed significant correlations between protein expression levels and the cognate mRNA levels of CPS (rho=0.520; p=0.01), SI (rho=0.900; p=0.037), I-FABP (rho=0.482; p=0.015), and L-FABP (rho=0.591; p=0.001), but not of GLUT5.

Two isoforms of the CPS protein were detected using these polyclonal antibodies, as described earlier (Figure 3B; Gaasbeek Janzen et al. 1984). CPS protein levels were significantly decreased on days 3–6, whereas CPS protein was significantly increased compared with controls on days 8–10, in accordance with the changes in mRNA levels (Figures 4A and 4C). SI protein levels were 50% decreased during days 1–2, parallel to the decreased mRNA levels, and remained decreased on days 3–4. SI protein was increased to control levels on days 5–10 (Figure 4C).

I-FABP and L-FABP protein levels tended to decrease compared with controls from day 3 onwards, but only L-FABP protein decreased significantly on days 5–6 (Figure 4C). On days 8–10, expression of both FABP protein levels was not statistically different from controls. As shown in Figure 4C, GLUT5 protein levels tended to increase during the early phase of damage on days 1–2, but levels were dramatically decreased on days 3–4 compared with controls. During regeneration, GLUT5 protein expression was rapidly increased, as it was in the range of control levels on days 5–10, in line with GLUT5 mRNA expression (Figures 4A and 4C).

In goblet cells, protein levels were not significantly correlated with the levels of the encoding mRNAs. MUC2 as well as TFF3 protein levels were significantly increased during all phases of damage despite the reduced mRNA levels (Figures 4B and 4D). In contrast to MUC2, TFF3 protein remained significantly elevated on days 8–10. Despite the overall similarity in response to MTX, there was no significant correlation between Muc2 and TFF3 protein levels, based on the analysis of the data from the individual rats.

Discussion

The loss of small intestinal epithelial cells and the occurrence of villous atrophy caused by MTX has been well described and has been appreciated since the 1970s (Altmann 1974; Jeynes and Altmann 1978). The unexpected diversity in our study regarding temporal expression patterns of 10 epithelial gene products in response to MTX indicates the involvement of specific regulation distinct and independent from extensive cell loss.

There are strong indications from our results and from previously published data (Taminiau et al. 1980; Kralovanszky and Prajda 1985; Tanaka et al. 1998) that glucose absorption is severely impaired during MTX-induced damage owing to the absence of important proteins, thereby contributing to malabsorption symptoms. SI and SGLT1 contribute to the digestion of starch and the absorption of glucose, the primary carbohydrate sources in the diet of the rats in our study. Because both SI and SGLT1 were significantly decreased during damage, these glucose-based energy sources cannot be efficiently utilized. The physiological importance of the absence of carbohydrate digestion and absorption is underscored by the loss of body weight that occurs up to day 4 after MTX treatment (Verburg et al. 2000).

Decreased expression of SGLT1 mRNA during damage is in agreement with previous findings using 5-FU as cytostatic drug (Tanaka et al. 1998). However, our data also demonstrated that SGLT1 mRNA was still significantly decreased during regeneration on days 5–6, when the length of the intestinal villi and the morphology of the epithelial cells appeared normal. At this time the epithelium was still in a higher proliferative state than controls (Verburg et al. 2000). Most likely, decreased SGLT1 expression was a result of incomplete differentiation of enterocytes. As a consequence, absorption of free glucose and sodium by SGLT1 was very likely impaired during damage as well as during regeneration. Defects in sodium absorption probably contribute to the development of diarrhea, which occurs during days 2–6 after MTX treatment (Verburg et al. 2000).

Glycohydrolase expression, measured by SI and lactase mRNA and SI protein, was significantly correlated with villous height. The decreased expression of these brush border proteins during villous damage confirms previous findings (Taminiau et al. 1980; Kralovanszky and Prajda 1985). The significant correlation between SI protein and mRNA indicates that SI expression was primarily transcriptionally regulated, in agreement with previous work on SI gene regulation (Traber et al. 1992; Krasinski et al. 1994).

GLUT5 is responsible for the uptake of fructose. Fructose, which was absent from the diet in the present study, induces GLUT5 mRNA and protein expression (Corpe et al. 1998). GLUT5 mRNA and protein expression levels were significantly decreased only during the phase of severe villous damage. If fructose were added to the diet as a carbohydrate source, it could have have stimulatory effects on GLUT5 expression during intestinal damage and regeneration, which could contribute to energy uptake to prevent malnourishment in the MTX-treated rat.

The strong correlation between crypt depth and CPS mRNA expression was in line with the fact that CPS mRNA is expressed exclusively by crypt enterocytes, whereas the protein is also found in villous enterocytes (Van Beers et al. 1998). The time lag between the decrease in CPS mRNA and protein levels can also be explained by their different localization pattern along the crypt–villous axis. A role for this mitochondrial protein in the intestinal urea cycle has been demonstrated by Davis and Wu (1998). These authors showed, in post-weaning pig enterocytes, that CPS favors the net synthesis of citrulline from ammonia, HCO_3^-, and ornithine. Thus far, a contribution of intestinal CPS to the systemic nitrogen balance by the consumption of ammonia may be underestimated compared to hepatic CPS. Our findings, however, could explain the reported hyperammonemia of patients treated with cytostatic drugs (Fine et al. 1989; Liaw et al. 1993).

Several functions have been reported for the cytosolic fatty acid-binding proteins in epithelial cells, as reviewed by Storch and Thumser (2000). Their role in the uptake and transport of fatty acids is important in

the regulation of cell membrane fatty acid levels and intracellular fatty acid concentrations that modulate fatty acid-responsive genes. Despite the relative slow recovery during regeneration, the expression of I-FABP and L-FABP mRNAs and proteins was the least affected among the panel of our enterocyte markers during the phase of crypt damage and villous damage. This was underscored using immunohistochemistry. Thus, the FABPs were relatively resistant to damage compared with carbohydrate-metabolizing enzymes and transporters and are probably important for maintaining membrane integrity and fatty acid absorption in villous enterocytes. This indicates that fatty acids are potentially important as an energy source for use during cytostatic drug treatment. The strong correlation between I-FABP and L-FABP gene expression suggests that both genes were co-ordinately regulated under this physiological state. Furthermore, because of the strong correlations between mRNA and protein levels, expression of both FABP proteins appeared transcriptionally regulated after MTX treatment.

In general, the presence and functionality of goblet cells and Paneth cells were preserved during the MTX-induced pathology. The expression patterns of MUC2, TFF3, and lysozyme indicated a generally enhanced secretion of cytoprotective molecules by goblet cells and Paneth cells during MTX-induced damage. Secretion of mucin and trefoil factor molecules is known to contribute to protection of the epithelium via a mucous layer (MUC2) and by promoting epithelial restitution (TFF3) (Dignass et al. 1994). During all phases of damage (days 1–4) the observed changes in goblet cell-specific mRNA expression did not reflect the changes in protein expression either for MUC2 or for TFF3. At early time points (days 1–2), the stable MUC2 and TFF3 mRNA expression was associated with highly increased protein expression. During villous atrophy (days 3–4), the decreased MUC2 and TFF3 mRNA expression was associated with increased protein expression. The reduced mRNA levels and increased protein levels can be explained by the loss of epithelial goblet cells, as we previously described (Verburg et al. 2000), and the involvement of post-transcriptional regulatory mechanisms that allow enhanced secretion of mucin and trefoil factor molecules. However, it is in contrast with the observation of Xian and colleagues, who reported no significant changes in TFF3 mRNA expression and significant decreased TFF3 protein expression in the proximal jejunum of MTX-treated rats during damage (Xian et al. 1999). Technically, the study of Xian et al. was performed differently by giving three SC injections of MTX, using different antibodies against TFF3, and using ribonuclease protection assays instead of Northern blots for analysis of mRNA expression. In addition, these authors had selected for another small intestinal region and another rat strain (Sprague–Dawley). They did not detect TFF3 protein during maximal damage, either immunohistochemically or on Western blotting, in contrast to our findings. Therefore, it is most likely that the intensity of damage was more severe in the study of Xian et al., leading to a much more decreased goblet cell function than in our study.

Despite the overall similarities in MUC2 and TFF3 protein and mRNA levels, no significant correlations were found in their levels of gene expression during MTX-induced damage and regeneration. This suggests that both genes were not co-ordinately regulated in goblet cells in response to chemotherapeutic damage, confirming recent work of others (Matsuoka et al. 1999).

The defense provided by Paneth cells is likely to act locally in the crypt micro-environment, e.g., in the area of the stem cells, via the secretion of a variety of crypt defensins and peptides that enhance innate mucosal immunity (Wilson et al. 1999). The MTX-induced increase in lysozyme mRNA expression and lysozyme immunostaining, seen on days 1–2 confirmed our previous findings (Verburg et al. 2000) and probably represents an adaptive response in Paneth cells to contribute to increased protection, during the vulnerable stages of the crypt epithelium.

In our study, an unexpected diversity in responses to MTX was observed between the 10 epithelial gene products. In particular, the remaining villous enterocytes during villous atrophy show a markedly specific response regarding their gene expression. These moribund cells appear to go through a programmed set of events that may be destined to maintain optimal epithelial performance during this stressed situation. Clinically, it may be possible to take advantage of these pre-programmed decisions by the absorptive epithelial cells to maintain optimal nutritional status in patients treated with cytostatic drugs. The central importance of the epithelial barrier function and the ability to regenerate after serious insults is reflected by the response of goblet cells and Paneth cells, in producing mucus, trefoil peptides and bactericidal peptides. The intestine thus reacts very specifically and diversely to severe damage or noxes and it appears very important to understand the different mechanisms involved in order to tailor enteral nutrition for patients treated with cytostatic drugs.

Acknowledgments

Supported by Numico BV, Wageningen, the Netherlands.

We thank Dr W.H. Lamers for the CPS probe and antibodies, and Dr S. Krasinsky for providing the SI probe. Dr K.Y. Yeh and Dr A. Quaroni are gratefully acknowledged for supplying anti-sucrase antibodies. Furthermore, we

thank Dr C.F. Burant for kindly providing SGLT1 and GLUT5 probes, and Dr B. Hirayama for his valued SGLT1 antibodies. Dr D. Yver kindly provided anti-GLUT5 antibodies. The I-FABP and L-FABP probes and antibodies were a generous gift from Dr J.I. Gordon. Dr D.K. Podolsky is acknowledged for providing both the TFF3 probe and the anti-TFF3 antibodies and Dr J.H. Power for providing the lysozyme probe. We also thank Dr K. Redekop for statistical advice and support.

Literature Cited

Alpers DH, Strauss AW, Ockner RK, Bass NM, Gordon JI (1984) Cloning of a cDNA encoding rat intestinal fatty acid binding protein. Proc Natl Acad Sci USA 81:313–317

Altmann GG (1974) Changes in the mucosa of the small intestine following methotrexate administration or abdominal x-irradiation. Am J Anat 140:263–279

Booth D, Haley JD, Bruskin AM, Potten CS (2000) Transforming growth factor-B3 protects murine small intestinal crypt stem cells and animal survival after irradiation, possibly by reducing stem-cell cycling. Int J Cancer 86:53–59

Booth D, Potten CS (2001) Protection against mucosal injury by growth factors and cytokines. J Natl Cancer Inst Monogr 29:16–20

Büller HA, Kothe MJC, Goldman DA, Sasak WV, Matsudaira PT, Montgomery RK, Grand RJ (1990) Coordinate expression of lactase-phlorizin hydrolase mRNA and enzyme levels in rat small intestine during development. J Biol Chem 265:6978–6983

Burant CF, Flink S, DePaoli AM, Chen J, Lee WS, Hediger MA, Buse JB, Chang EB (1994) Small intestine hexose transport in experimental diabetes. Increased transporter mRNA and protein expression in enterocytes. J Clin Invest 93:578–585

Corpe CP, Bovelander FJ, Hoekstra JH, Burant CF (1998) The small intestinal fructose transporters: site of dietary perception and evidence for diurnal and fructose sensitive control elements. Biochim Biophys Acta 1402:229–238

Davis PK, Wu G (1998) Compartmentation and kinetics of urea cycle enzymes in porcine enterocytes. Comp Biochem Physiol [B] 119:527–537

Dignass A, Lynch–Devaney K, Kindon H, Thim L, Podolsky DK (1994) Trefoil peptides promote epithelial migration through a transforming growth factor beta-independent pathway. J Clin Invest 94:376–383

Fata F, Ron IG, Kemeny N, O'Reilly E, Klimstra D, Kelsen DP (1999) 5-fluorouracil-induced small bowel toxicity in patients with colorectal carcinoma. Cancer 86:1129–1134

Fine P, Adler K, Gerstenfeld D (1989) Idiopathic hyperammonemia after high-dose chemotherapy. Am J Med 86:629

Gaasbeek Janzen JW, Lamers WH, Moorman AF, de Graaf A, Los JA, Charles R (1984) Immunohistochemical localization of carbamoyl-phosphate synthetase (ammonia) in adult rat liver; evidence for a heterogeneous distribution. J Histochem Cytochem 32:557–564

Goldman ID, Matherly LH (1985) The cellular pharmacology of methotrexate. Pharmacol Ther 28:77–102

Gordon JI, Alpers DH, Ockner RK, Strauss AW (1983) The nucleotide sequence of rat liver fatty acid binding protein mRNA. J Biol Chem 258:3356–3363

Hirano M, Iwakiri R, Fujimoto K, Sakata H, Ohyama T, Sakai T, Joh T, et al. (1995) Epidermal growth factor enhances repair of rat intestinal mucosa damaged by oral administration of methotrexate. J Gastroenterol 30:169–176

Howarth GS, Cool JC, Bourne AJ, Ballard FJ, Read LC (1998) Insulin-like growth factor-I (IGF-I) stimulates regrowth of the damaged intestine in rats, when administered following, but not concurrent with, methotrexate. Growth Factors 15:279–292

Hwang ES, Hirayama BA, Wright EM (1991) Distribution of the SGLT1 Na+/glucose cotransporter and mRNA along the crypt-villus axis of rabbit small intestine. Biochem Biophys Res Commun 181:1208–1217

Jeynes BJ, Altmann GG (1978) Light and scanning electron microscopic observations of the effects of sublethal doses of methotrexate on the rat small intestine. Anat Rec 191:1–17

Keefe DM, Brealey J, Goland GJ, Cummins AG (2000) Chemotherapy for cancer causes apoptosis that precedes hypoplasia in crypts of the small intestine in humans. Gut 47:632–637

Kohout P, Cerman J, Bratova M, Zadak Z (1999) Small bowel permeability in patients with cytostatic therapy. Nutrition 15:546–549

Kralovanszky J, Prajda N (1985) Biochemical changes of intestinal epithelial cells induced by cytostatic agents in rats. Arch Toxicol Suppl 8:94–103

Krasinski SD, Estrada G, Yeh KY, Yeh M, Traber PG, Rings EH, Buller HA, et al. (1994) Transcriptional regulation of intestinal hydrolase biosynthesis during postnatal development in rats. Am J Physiol 267:G584–594

Liaw CC, Liaw SJ, Wang CH, Chiu MC, Huang JS (1993) Transient hyperammonemia related to chemotherapy with continuous infusion of high-dose 5-fluorouracil. Anticancer Drugs 4:311–315

Matsuoka Y, Pascall JC, Brown KD (1999) Quantitative analysis reveals differential expression of mucin (MUC2) and intestinal trefoil factor mRNAs along the longitudinal axis of rat intestine [in process citation]. Biochim Biophys Acta 1489:336–344

Nyunoya H, Broglie KE, Widgren EE, Lusty CJ (1985) Characterization and derivation of the gene coding for mitochondrial carbamyl phosphate synthetase I of rat. J Biol Chem 260:9346–9356

Petschow BW, Carter DL, Hutton GD (1993) Influence of orally administered epidermal growth factor on normal and damaged intestinal mucosa in rats. J Pediatr Gastroenterol Nutr 17:49–58

Pinkerton CR, Cameron CH, Sloan JM, Glasgow JF, Gwevava NJ (1982) Jejunal crypt cell abnormalities associated with methotrexate treatment in children with acute lymphoblastic leukaemia. J Clin Pathol 35:1272–1277

Podolsky DK, Fournier DA, Lynch KE (1986) Development of anti-human colonic mucin monoclonal antibodies. Characterization of multiple colonic mucin species. J Clin Invest 77:1251–1262

Potten CS, Owen G, Hewitt D, Chadwick CA, Hendry H, Lord BI, Woolford LB (1995) Stimulation and inhibition of proliferation in the small intestinal crypts of the mouse after in vivo administration of growth factors. Gut 36:864–873

Quaroni A, Isselbacher KJ (1985) Study of intestinal cell differentiation with monoclonal antibodies to intestinal cell surface components. Dev Biol 111:267–279

Rand EB, Depaoli AM, Davidson NO, Bell GI, Burant CF (1993) Sequence, tissue distribution, and functional characterization of the rat fructose transporter GLUT5. Am J Physiol 264:G1169–1176

Rings EH, Krasinski SD, van Beers EH, Moorman AF, Dekker J, Montgomery RK, Grand RJ, et al. (1994) Restriction of lactase gene expression along the proximal-to-distal axis of rat small intestine occurs during postnatal development. Gastroenterology 106:1223–1232

Rubin DC, Ong DE, Gordon JI (1989) Cellular differentiation in the emerging fetal rat small intestinal epithelium: mosaic patterns of gene expression. Proc Natl Acad Sci USA 86:1278–1282

Storch J, Thumser AE (2000) The fatty acid transport function of fatty acid-binding proteins. Biochim Biophys Acta 1486:28–44

Suemori S, Lynch–Devaney K, Podolsky DK (1991) Identification and characterization of rat intestinal trefoil factor: tissue- and cell-specific member of the trefoil protein family. Proc Natl Acad Sci USA 88:11017–11021

Taminiau JA, Gall DG, Hamilton JR (1980) Response of the rat small-intestine epithelium to methotrexate. Gut 21:486–492

Tanaka H, Miyamoto KI, Morita K, Haga H, Segawa H, Shiraga T, Fujioka A, et al. (1998) Regulation of the PepT1 peptide transporter in the rat small intestine in response to 5-fluorouracil-induced injury. Gastroenterology 114:714–723

Traber PG, Yu L, Wu GD, Judge TA (1992) Sucrase-isomaltase gene expression along crypt-villus axis of human small intestine is regulated at level of mRNA abundance. Am J Physiol

262:G123–130
Tytgat KM, Bovelander FJ, Opdam FJ, Einerhand AWC, Büller HA, Dekker J (1995a) Biosynthesis of rat MUC2 in colon and its analogy with human MUC2. Biochem J 309:221–229
Tytgat KM, Klomp LW, Bovelander FJ, Opdam FJ, Van der Wurff A, Einerhand AWC, Büller HA, et al. (1995b) Preparation of anti-mucin polypeptide antisera to study mucin biosynthesis. Anal Biochem 226:331–341
Van Beers EH, Rings EH, Posthuma G, Dingemanse MA, Taminiau JA, Heymans HS, Einerhand AW, et al. (1998) Intestinal carbamoyl phosphate synthase I in human and rat. Expression during development shows species differences and mosaic expression in duodenum of both species. J Histochem Cytochem 46:231–240
Verburg M, Renes IB, Meijer HP, Taminiau JA, Büller HA, Einerhand AW, Dekker J (2000) Selective sparing of goblet cells and paneth cells in the intestine of methotrexate-treated rats. Am J Physiol 279:G1037–1047
Werkheiser WC (1961) Specific binding of 4-amino folic acid analogues by folic acid reductase. J Biol Chem 236:888–893
Wilson CL, Ouellette AJ, Satchell DP, Ayabe T, Lopez-Boado YS, Stratman JL, Hultgren SJ, et al. (1999) Regulation of intestinal alpha-defensin activation by the metalloproteinase matrilysin in innate host defense. Science 286:113–117
Xian CJ, Howarth GS, Mardell CE, Cool JC, Familari M, Read LC, Giraud AS (1999) Temporal changes in TFF3 expression and jejunal morphology during methotrexate-induced damage and repair. Am J Physiol 277:G785–795
Yeh KY, Yeh M, Holt PR (1991) Thyroxine and cortisone cooperate to modulate postnatal intestinal enzyme differentiation in the rat. Am J Physiol 260:G371–378
Yogalingam G, Doyle IR, Power JH (1996) Expression and distribution of surfactant proteins and lysozyme after prolonged hyperpnea. Am J Physiol 270:L320–330
Yoshida A, Takata K, Kasahara T, Aoyagi T, Saito S, Hirano H (1995) Immunohistochemical localization of Na(+)-dependent glucose transporter in the rat digestive tract. Histochem J 27:420–426